Combustion of Methane and Biogas Fuels in Gas Turbine Can-type Combustor Model

A. Guessab[1†], A. Aris[1], M. Cheikh[2] and T. Baki[2]

[1] *Mechanical Engineering Department, ENPO, 31000 Oran, Algeria.*
[2] *Mechanical Engineering Department, USTOMB, Oran, 31000, Algeria.*

†*Corresponding Author Email: ahmed.guessab@enp-oran.dz*

ABSTRACT

The paper presents the numerical simulation on combustion of methane and biogas mixtures in the swirl burner can-Type of gas turbine combustion chamber. The study deals with the impact of mass fraction of carbon dioxide for biogas on emissions of noxious compounds during combustion. The investigations were done for four different fuels: pure methane (100% CH_4), three biogases ($90\%CH_4+10\%CO_2$, $75\%CH_4+25\%CO_2$ and $70\%CH_4+30\%CO_2$), with the constant value of equivalence ratio ($\phi = 0.95$). The numerical results show that a low content of carbon dioxide in methane-air mixture leads to a better flame stability through an increase of the volume of the recirculation zone. The numerical analysis has shown that the biogas fuel allows a reduction of about 33% on the NO emissions and about 10% on the CO emissions and carbon dioxide contained in the fuel leads to the lowering of the flame temperature, whose effect reduces NO emissions. The results of the investigation clearly demonstrate that it is possible to use such fuels in combustion systems with swirl burners.

Keywords: Methane; Biogas; Swirl combustor; NO.

1. INTRODUCTION

The turbines are widely used in modern industry to deliver shaft power or thrust power. The combustor is part of the gas turbine. The main goal of the combustor design is lower emissions with less volume. Flow field simulation in the combustor is a challenging subject to both academics and industries. It is of commercial importance to understand and to predict various phenomena in the combustor.

Gas turbine combustion systems need to be designed and developed to meet many mutually conflicting design requirements, including high combustion efficiency over a wide operating envelope and low NO_x emission, low smoke, low lean flame stability limits and good starting characteristics; low combustion system pressure loss, low pattern factor, and sufficient cooling air to maintain low wall temperature levels and gradients commensurate with structural durability.

Swirling flames are frequently used in modern gas turbine combustors since they offer a possibility of controlled flame temperature and thus favorable thermal NO_x emissions.

Emissions of nitrogen oxides (NO_x), which are responsible in particular pollutant photochemical formation of ground-level zone and acid rain, have a significant environmental impact and health. very strict standards to limit these emissions are currently in force in particular for stationary sources (industrial burners, thermal power plants, boilers,...) and for mobile sources (vehicle engines, aircraft,...). NO_x are essentially the combustion by-products. among the denitrification processes, alternative technologies reburn advanced (R.A.), which combine reburn processes (natural gas) Reduction and Selective Non catalytic (S.N.C.R.) (by nitrogen species) are currently being validated on an industrial scale (Gohlke, 2010), (Rossignoli, 2010), (White, 2009).

Numerical simulations of the flows in gas turbine combustors had become an unavoidable way to accelerate the design of this type of modern engines and optimize their performances. The calculations also facilitate the understanding and the visualization of physical phenomena often inaccessible by the experimental measurements.

Biogas can be used readily in all applications designed for natural gas such as direct combustion including absorption heating and cooling, cooking, space and water heating, drying, and gas turbines. It may also be used in fueling internal combustion engines and fuel cells for production of mechanical work and/or electricity. If cleaned up to

adequate standards is may be injected into gas pipelines and provide illumination and steam production.

The addition of CO_2 to natural gas fuel affects both the chemical and physical processes occurring in flames. These changes affect flame stability, pollutant emissions and combustion efficiency. Few of these issues are clearly understood.

The use of Computational Fluid Dynamics codes to predict the reactive flow within a gas turbine combustor has been the center of many studies, made improvements to the accuracy of emissions predictions and combustor simulation: (Lysenko and Solomatnikov, 2003, 2006); Palm *et al.* (2006); Fureby *et al.* (2007); Widenhorn *et al.* (2009); (2010); Pathan *et al.* (2012); Ghenai (2010), Eldrainy *et al.* (2008).

This project will investigate issues surrounding the use of methane and biogas fuels in gas turbines. The influence of the addition of CO_2 to natural gas on the stability of turbulent flames is investigated in this numerical project.

Combustion in gas turbines combustor predominantly takes place in the diffusion flame regime and in the thin-reaction zones regime. The main goal of this project is to develop improved turbulent combustion models for circumstances in gas turbines can-type combustor model, including accurate chemistry and improved turbulence modeling.

The present analysis is mainly based on three-dimensional Steady Reynolds Averaged Navier-Stokes equations, employing Reynolds Stress Model as the turbulence model. In this works the version of RSM due to Speziale, Sarkar (1995), Sarkar and Gatski (1991) and Marzougui *et al.* (2015), has been selected, since it applies a quadratic correlation for modeling the isotropization of production in the pressure-strain tensor. Numerical simulations were performed with the commercial code FLUENT 14.0 by ANSYS Inc.

The Eddy Dissipation Model (EDM) by Magnussen (2005) was taken into account to model turbulence/chemistry interactions. Two-step global mechanism of Westbrook and Dryer (1981) was used to describe the oxidation of Methane/Biogas.

In laminar flames and at the molecular level within turbulent flames, the formation of NO_x can be attributed to four distinct chemical kinetic processes: thermal NO_x formation, prompt NO_x formation, fuel NO_x formation, and intermediate N_2O. Thermal NO_x is formed by the oxidation of atmospheric nitrogen present in the combustion air. Prompt NO_x is produced by high-speed reactions at the flame front (DeSoete, 1974). Fuel NO_x is produced by oxidation of nitrogen contained in the fuel. At elevated pressures and oxygen-rich conditions, NO_x may also be formed from molecular nitrogen (N_2) via N_2O. The reburning and the Selective Non-Catalytic

Reduction (SNCR) mechanisms reduce the total NO_x formation by accounting for the reaction of NO with hydrocarbons and ammonia, respectively.

The aim of the current work is: (1) Study the rate constants in the ANSYS Fluent NO formation model, (2) Choosing biogas as a fuel in gas turbine combustion chamber.

2. COMBUSTOR MODELING

2.1 Geometry and Grid

The basic geometry of the gas turbine can-type combustion chamber is shown in Fig. 1. The size of the combustor is 590 mm in the Z direction, 250 mm in the Y direction, and 230 mm in the X direction. The primary inlet air is guided by vanes to give the air a swirling velocity component. The total surface area of primary main air inlet is 57 cm^2. The fuel is injected through six fuel inlets in the swirling primary air flow. There are six small fuel inlets, each with a surface area of 0.14 cm^2. The secondary air is injected in the combustion chamber through six side air inlets each with an area of 2 cm^2. The secondary air or dilution air is injected at 0.1 m from the fuel injector to control the flame temperature and NO_x emissions. The can-type combustor outlet has a rectangular shape with an area of 0.0150 m^2.
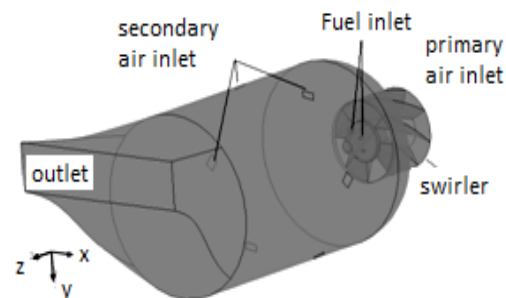

Fig. 1. Model combustor: computational domain model.

2.2 Boundary Conditions and Meshing

In the present study, unstructured grid has been employed due to the complexity of geometry combustor. An unstructured grid was generated with GAMBIT, illustrated in Fig. 2, which consists of 45,568 nodes and 110,568 elements. The different boundary conditions applied for this numerical simulation of gas turbine can-type combustion chamber are listed in Table 1. The Finite Volume Method (Eymard *et al.*, 2000) and the second-order upwind method were used to solve the governing equations. The convergence criteria were set to 10^{-4} for the mass, momentum, turbulent kinetic energy and the dissipation rate of the turbulent kinetic energy and the chemical species conservation equations. For the energy and the pollution equations, the convergence criteria were set to 10^{-6}.
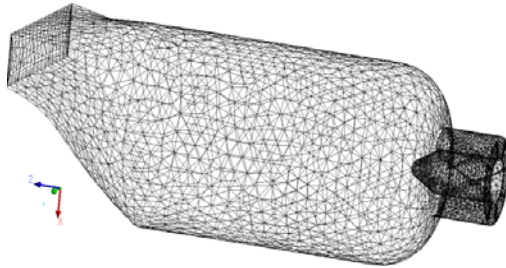
Fig. 2. Computational mesh.

Table 1 boundary conditions

Primary air	Flow regime: subsonic; The injection velocity is 10m/s The injector diameter is 85mm Heat transfer: static temperature is 300K The turbulence intensity is 10% Mass fraction of oxygen: Y_{O2}= 0.232;
Fuel inlet	Flow direction: normal to B. C. Flow regime: subsonic; The injection velocity is 40 m/s The injector diameter is 4.2 m The temperature is 300 K; Thermal radiation: local temperature;
Sec. air	The injection velocity is 6m/s; The injector diameter is 16mm The temperature is 300K The turbulence intensity is 10% Mass fraction of oxygen: Y_{O2}= 0.232
Outlet	Flow regime: subsonic; The relative pressure is 0Pa; Mass fraction of oxygen: Y_{O2}= 0.232 Thermal radiation: local temperature;
Wall	Wall boundary condition was no slip; Wall roughness was smooth; Wall heat transfer was adiabatic; Wall emissivity was 0.95; Thermal radiation: opaque; Diffuse fraction is 1.0

2.3 Turbulent Combustion Modeling

For turbulence modeling, it is already known, that certain Reynolds Stress components are significantly modified due to the action of flow curvature and pressure gradient within swirling flows. Consequently, eddy viscosity models, which do not address such phenomena, perform badly. Such phenomena can however be accommodated within a Reynolds Stress Model (RSM) closure.

The Reynolds stress model (RSM) is the most elaborate type of RANS turbulence model that ANSYS FLUENT provides. Abandoning the isotropic eddy-viscosity hypothesis, the RSM closes the Reynolds-averaged Navier-Stokes equations by solving transport equations for the Reynolds stresses, together with an equation for the dissipation rate. This means that five additional transport equations are required in 2D flows, in comparison to seven additional transport equations solved in 3D. Since the RSM accounts for the effects of streamline curvature, swirl, rotation, and rapid changes in strain rate in a more rigorous manner than one-equation and two-equation models, it has greater potential to give accurate

predictions for complex flows. However, the fidelity of RSM predictions is still limited by the closure assumptions employed to model various terms in the exact transport equations for the Reynolds stresses. The modeling of the pressure-strain and dissipation-rate terms is particularly challenging, and often considered to be responsible for compromising the accuracy of RSM predictions. In addition, even RSM rely on scale equations (ε or ω) and inherit deficiencies resulting from the underlying assumptions in these equations.

The RSM might not always yield results that are clearly superior to the simpler models in all classes of flows to warrant the additional computational expense. However, use of the RSM is a must when the flow features of interest are the result of anisotropy in the Reynolds stresses. Among the examples are cyclone flows, highly swirling flows in combustors, rotating flow passages, and the stress-induced secondary flows in ducts. The exact form of the Reynolds stress transport equations may be derived by taking moments of the exact momentum equation. This is a process wherein the exact momentum equations for the fluctuations are multiplied by the fluctuating velocities and averaged, the product then being Reynolds-averaged. Unfortunately, several of the terms in the exact equation are unknown and modeling assumptions are required in order to close the equations.

In this project, the Eddy Dissipation Model (EDM) of Magnussen (2005) is used as the interaction between turbulence and combustion. The Eddy Dissipation model is best applied to turbulent flows when the chemical reaction rate is fast relative to the transport processes in the flow. There is no kinetic control of the reaction process. Thus, ignition and processes where chemical kinetics may limit reaction rate may be poorly predicted. By default, for the Eddy Dissipation Model (EDM); requires that fuel and oxidant are produced in adequate volume so that the combustion occurs. If the product limiter is enabled, by setting the Eddy Dissipation Coefficient B parameter to positive, then products must also be available. For more details, see (Magnussen, 2005). However, combustion products may not always be specified as an input. In this case, products could not form unless they are introduced into the domain. Assuming the problem is one in which a stable flame may be established, initial specification of products within the domain should be sufficient to start and maintain combustion. However, if the combustion is difficult to maintain, it may be necessary to introduce a small fraction of products at an inlet.

The eddy dissipation model is based on the concept that chemical reaction is fast relative to the transport processes in the flow. When reactants mix at the molecular level, they instantaneously form products. The model assumes that the reaction rate may be related directly to the time required to mix reactants at the molecular level. In turbulent flows, this mixing time is dominated by the eddy properties and, therefore, the rate is proportional to

a mixing time defined by the turbulent kinetic energy, k, and dissipation, ε.

$$rate \propto \frac{\varepsilon}{k} \tag{1}$$

This concept of reaction control is applicable in many industrial combustion problems where reaction rates are fast compared to reactant mixing rates.

In the Eddy Dissipation model, the rate of progress of elementary reaction k, is determined by the smallest of the two following expressions:

$$R_k = A \frac{\varepsilon}{k} \min\left(\frac{[I]}{\nu_{kI'}}\right) \tag{2}$$

where A is a constant value, $[I]$ the molar concentration of component I and I only includes the reactant components and $\nu_{\varepsilon I'}$ the exponent of species I for the reactant side. of the products limiter is preferred, the equation results:

$$R_k = A B \frac{\varepsilon}{k} \left(\frac{\sum_P (I W_I)}{\sum_P \nu_{kI'} W_I}\right) \tag{3}$$

where

P loops over all product components in the elementary reaction k.
A is a an empirical constant equal to 4.0
B is an empirical constant equal to 0.5;
ε is the turbulent dissipation rate (m^{2}s^{-3});
K is the turbulent kinetic energy per unit mass (J/kg).
ν'_i, ν''_j is the stoichiometric coefficient for reactant i and product j in reaction.

Optionally, a maximum flame temperature may be applied for the Eddy Dissipation model. The reaction rate is smoothly blended to zero when the specified upper temperature limit is approached. This is implemented by an additional bound added to the minimum condition in the EDM reaction rate:

$$R_{k,MFT} = A \frac{\varepsilon}{k} C_{MFT} \tag{4}$$

Where:

$$C_{MFT} = \max\left\{(T_{max} - T), 0[K]\right\} \cdot \frac{\rho C_p}{\Delta H_R} \tag{5}$$

C_{MFT} may be interpreted as a virtual concentration, which vanishes if the temperature is equal to the maximum flame temperature. C_p is the specific heat capacity of the fluid mixture at constant pressure and ΔH_R is the reaction heat release per mole.

The assumption made for the EDM no longer holds true when one chemistry time scale becomes relevant. However, the limits of application of the EDM can be extended by combining it with the Finite Rate Chemistry (FRC) model, in which the reaction rates are calculated by means of a chemical kinetic mechanism:

$$R_{SFRC} = F_S \prod_{I=X_1,X_2,\dots}^{N_s} [I]^{\nu SI'} - B_S \prod_{I=X_1,X_2,\dots}^{N_s} [I]^{\nu SI''} \tag{6}$$

F_s and B_s are the forward and backward rate constants, which are calculated through an Arrhenius like expression. According to the local conditions, the overall model (EDM-FRC) switches between the reaction rates calculated with the EDC or the FRC model.
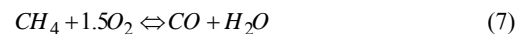
Although the boundaries of applicability of the EDM model are clearly expanded by adding Finite Rate Chemistry effects, there is still a clear limit to the model due to the very simple chemical kinetics schemes which can be adopted in this context. Normally the schemes which are supported in this numerical technique are single step global reaction schemes.

The reaction chemistry is a simple infinitely fast one step global irreversible reaction. The model for the reaction rate is developed from a combination of local kinetics modeling using an Arrhenius law and a new form of the EDC model adapted for LES. The modeling can in principle be applied to both premixed and non-premixed flame and can easily be extended for more complex chemistry. The investigations were done for four different fuels: pure methane, three biogases, with the constant value of equivalence ratio ϕ = 0.95. The composition of the gases tested is presented in Table 2.

Table 2 Fuel mixtures

	%Ch$_4$	%CO$_2$	Low Heat Value, MJ/m^3
Methane	100	0	36
Biogas 1	90	10	32.4
Biogas 2	75	25	27
Biogas 3	70	30	25.2

For methane and biogas flame calculations, a general 2-step chemistry by Westbrook and Dryer (1984) for saturated hydrocarbon fuels is used. The two steps are:

$$CH_4 + 1.5O_2 \Leftrightarrow CO + H_2O \tag{7}$$

$$CO + 0.5O_2 \Rightarrow CO_2 \tag{8}$$

2.4 NO$_x$ Formation

There are two mechanisms that create NO$_x$ in gas turbine combustor: the Thermal NO$_x$, which is the oxidation of atmospheric bound nitrogen in the combustion air and the conversion of fuel, bound nitrogen into NO$_x$. The formation of thermal NO$_x$ is determined by a set of highly temperature-dependent chemical reactions known as the extended Zeldovich mechanism. The principal reactions governing the formation of thermal NO$_x$

from molecular nitrogen are as follows (Palash *et al.*, 2013):

$$O + N_2 \Leftrightarrow N + NO \tag{9}$$

$$N + O_2 \Leftrightarrow O + NO \tag{10}$$

A third reaction has been shown to contribute to the formation of thermal NOx, particularly at near-stoichiometric conditions and in fuel-rich mixtures:

$$N + OH \Leftrightarrow H + NO \tag{11}$$

The expressions for the rate coefficients for Eqs. 9, 10 and 11 used in the NOx model are given below. These were selected based on the evaluation of Hanson and Salimian (1984).

$$K_{f,1} = 1.8 \times 10^8 \exp\{-38370/T\} \tag{12}$$

$$K_{r,1} = 3.8 \times 10^7 \exp\{-425/T\} \tag{13}$$

$$K_{f,2} = 1.8 \times 10^4 \, T \exp\{-4680/T\} \tag{14}$$

$$k_{r,2} = 3.81 \times 10^3 \, T \exp\{-20820/T\} \tag{15}$$

$$k_{f,3} = 7.1 \times 10^7 \exp\{-450/T\} \tag{16}$$

$$k_{r,3} = 1.7 \times 10^8 \exp\{-24560/T\} \tag{17}$$

In the above expressions, $k_{f,1}$, $k_{f,2}$, and $k_{f,3}$ are the rate constants for the forward reactions Eqs. 6, 7 and 8, respectively, and $k_{r,1}$, $k_{r,2}$, and $k_{r,3}$ are the corresponding reverse rate constants. All of these rate constants have units of m^3/mol-s.

The net rate of formation of NO via the reactions in Eqs. 6, 7 and 8 is given by

$$\frac{d[NO]}{dt} = k_{f,1}[O][N_2] + k_{f,2}[N][O_2] + k_{f,3}[N][OH]$$
$$- k_{r,1}[NO][N] - k_{r,2}[NO][O] - k_{r,3}[NO][H] \tag{18}$$

were all concentrations have units of mol/m^3.

To determine the O radical concentration, ANSYS Fluent uses one of three approaches – the equilibrium approach, the partial equilibrium approach, and the predicted concentration approach. In this study uses the equilibrium approach. The kinetics of the thermal NOx formation rate is much slower than the main hydrocarbon oxidation rate, and so most of the thermal NOx is formed after completion of combustion. Therefore, the thermal NOx formation process can often be decoupled from the main combustion reaction mechanism and the NOx formation rate can be calculated by assuming equilibration of the combustion reactions. Using this approach, the calculation of the thermal NOx formation rate is considerably simplified.

The assumption of equilibrium can be justified by a reduction in the importance of radical overshoots at higher flame temperature. According to Westenberg (2009), the equilibrium O-atom concentration can be obtained from the expression

$$[O] = 3.97 \times 10^5 T^{-1/2} [O_2]^{1/2} e^{-31090/T} \quad [mol/m^3] \tag{19}$$

were T is in Kelvin.

ANSYS Fluent uses one of three approaches to determine the OH radical concentration of OH from the thermal NOx calculation approach, the partial equilibrium approach, and the use of the predicted OH concentration approach.

In this study, we used the partial equilibrium approach, in this approach, the concentration of OH in the third reaction in the extended Zeldovich mechanism (Eq. 8) is given by (Baulch *et al.,* 1992); (Westbrook and Dryer, 1984).

$$[OH] = 2.129 \times 10^2 T^{-0.57} e^{-4595/T} [O]^{1/2} [H_2O]^{1/2} \tag{20}$$

The presence of a second mechanism leading to NOx formation was first identified by Fenimore (1971) and was termed "prompt NOx ". There is good evidence that prompt NOx can be formed in a significant quantity in some combustion environments, such as in low-temperature, fuel-rich conditions and where residence times are short. Surface burners, staged combustion systems, and gas turbines can create such conditions.

At present, the prompt NOx contribution to total NOx from stationary combustion is small. However, as NOx emissions are reduced to very low levels by employing new strategies (burner design or furnace geometry modification), the relative importance of the prompt NOx can be expected to increase. More information can be found in ANSYS help. In turbulent combustion calculations, ANSYS FLUENT solves the density-weighted time-averaged Navier-Stokes equations for temperature, velocity, and species concentrations or mean mixture fraction and variance. To calculate concentration, a time-averaged formation rate must be computed at each point in the domain using the averaged flow-field information. Methods of modeling the mean turbulent reaction rate can be based on either moment methods or probability density function (PDF) techniques. ANSYS FLUENT uses the PDF approach.

3. RESULTS AND DISCUSSION

3.1 Velocity Streamline

Fig. 3, shows the streamline contours produced by the numerical model. The color of the streamline patterns represents the axial values of velocity. These streamlines indicate the path which a fluid particle would follow. Flame stability, combustion intensity, and performance are directly associated with the size and shape of this recirculation vortex.

In primary zone, the negative axial velocities in the center of the combustion chamber indicate the existence of an inner recirculation zone. Swirl vanes around the fuel nozzle generate a strong vortex flow in the combustion air within the combustor. The flow field is typical of confined swirl flames and consists of a cone-shaped stream of burning gas in the inlet of the chamber. For sufficiently high swirl

number (in this study, S=1.0), recirculation zone appears as a result of the vortex breakdown. The length of the recirculation zone is about (150 mm).
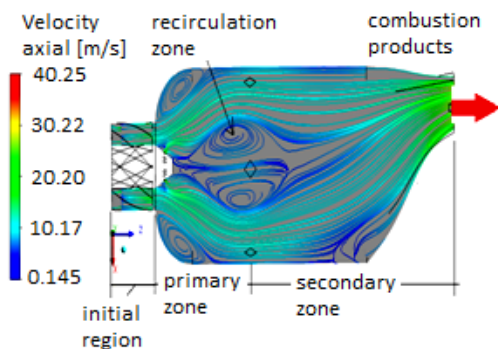

Fig. 3. Velocity streamline in meridian plan (Oxz).

The recirculation zone operates normally at a rich mixture. This recirculation region is deeply involved in the flame stabilization process as it constantly puts hot burnt gases in contact with fresh gases allowing permanent ignition. The central recirculation zone results from the vortex breakdown generated by the Swirl. This large torridly central recirculation zone plays a main role in the flame stabilization process by acting as a store for heat and chemically active species. Negative axial velocities in corner regions indicate the existence of two corner recirculation zones resulting from sudden expansion. Corner recirculation zone above the shear layer of the recirculation zone and takes it shape from the neighboring boundary walls.

The length of the corner recirculation zone is about (76 mm). Strong velocity gradients occur in the throat of the nozzle and, in the outer shear layer between inflow and recirculation zone, because of the strong turbulent mixing in those locations.

The secondary zone adds air to weaken the mixture. More air is added in the dilution zone to decrease the hot gas temperature for meeting the requirement of turbine guide vanes. This hot gas helps stabilize the flame by providing a continual source of ignition to the incoming fuel. It also serves as a zone of intense mixing within the combustion by promoting turbulence through high levels of shear between the forward and reverse flows. Recirculation zone is formed just at the downstream of the secondary air inlet.

Fuel velocity coming out from the injector at the plan 1 (Fig. 4) has a magnitude of 40m/s. Air coming through the swirly jet has a maximum velocity of 10 m/s and this flow spreads in the radial direction occupying whole space without formation of recirculation zone. This is due to the blockage effect created by the secondary air inlet jets forcing the primary air inlet jets and fuel jet to spread in radial direction. Velocity of fuel-air mixture reduces as I enter the liner axis of combustor.

From Fig. 4, it can be seen that the modeling of dilution holes (secairin) results in the corresponding air jets being generated. The secairin jets help in recirculation a part of the primary air to aid in combustion in the primary zone. This zone is a prerequisite for the stable combustion. The function of the dilution air jet is to mix with the products of combustion to cool these to a value acceptable by the turbine and also to reduce the pattern factor at the exit of the combustor.
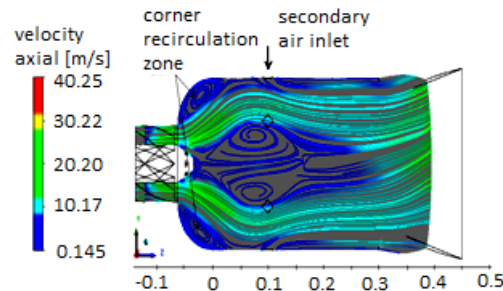

Fig. 4. Streamline of velocity field in combustor gas turbine, Horizontal section.

3.2 Combustion Aerodynamic

The design and performance of a combustor is strongly affected by aerodynamic processes. The achievement of aerodynamically efficient designs, characterized by good mixing and stable flow patterns with minimal parasitic losses, is one of the primary design objectives. Large scale central recirculation zones, as shown in Fig. 5, serve many other purposes as well.
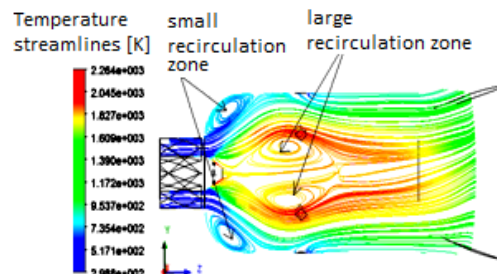

Fig. 5. The process of recirculation in a gas turbine combustor using temperature streamlines.

Swirlers are static mixing devices used to impart swirl to the flow. The goal of swirler design is to maximize the benefits of recirculation by imparting sufficient swirl to the flow while minimizing the incurred pressure losses. Modern combustors also use swirlers to promote mixing of the fuel and air in the premier prior to combustion. At swirled and injector fuel jet, temperature of inlet air and fuel (100% CH_4) was taken as 300K. After the initial region, temperature increases gradually from 300K to a maximum value of 2264K in the central region due to efficient combustion of fuel-air mixture. Hot combustion products become trapped in the recirculating mass and are returned to the combustor dome inlet. This hot gas helps stabilize

the flame by providing a continual source of ignition to the incoming fuel. Fig. 5 illustrates the process of recirculation in a gas turbine combustor using streamlines. These streamlines indicate the path which a fluid particle would follow.

The mixture flows axially after the reaction and it diffuses away from the center to ensure entrainment of more air along the centerline of the secondary zone of the combustor thereby reducing the temperature in this region. Outlet temperature contours are more uniform (T=1300K).

3.4 Effect of Fuel Characteristics (T, NO, CO_2)

Methane is used as the reference fuel. Waste biogas is composed of Biogas 1 (%CH_4=90, %CO_2=10), Biogas 2 (%CH_4=75, %CO_2=25) and Biogas 3 (%CH_4=70, %CO_2=30), with a constant velocity inlet of fuel and air. In the current studies, the vane angle was assumed to be about 45° and was kept constant for all the simulation. The simulations were validated in terms of temperature and emission of pollutants NO and CO_2. The temperature distribution along the central axis of combustor is shown in Fig. 6. As seen in the figure, due to more fuel burned under the increase percentage of CO_2, the outlet temperature decrease as the CO_2 increases. In the region from the fuel injector to z = 0.1m, the temperature at the central axis of combustor has little change for all fuels.
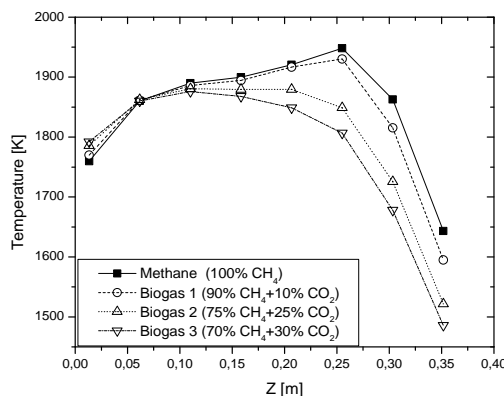
Fig. 6. Distribution of temperature.

However, in the region from 0.1 m to combustor outlet, the temperature decrease as the percentage of CO_2 increases. It can also be seen from Fig. 6 due to the air from the secondary holes takes more heat to reach the equilibrium temperature and the combustion process the mixing of dilution air and fuel gas is useful to improve the uniformity of combustor outlet temperature distribution. The temperature increases gradually due to the chemical reaction inside the main combustor. It is clear that after the location of primary chamber at z = 0.25m, the temperature diminishes due to the cooling effect of air from the secondary holes. Thus, it is distinct to show that for the biogas 3, achieves better temperature in comparison with other fuel. The peak gas temperature is located in the secondary zone (z = 0.25m) for methane and biogas 1. Then the peak gas temperature is located in the primary

zone for Biogas 2 and biogas 3 (z = 0.1m). Fig. 7 demonstrates the NO mass fraction for the can combustor model with different fuels at axial distance. The highest values of distribution of the mass fraction of NO in the combustor chamber were measured for fuels with the highest combustion temperature. NO concentrations, however, are highest in the slow-moving, reverse-flowing fluid near the combustor centerline.
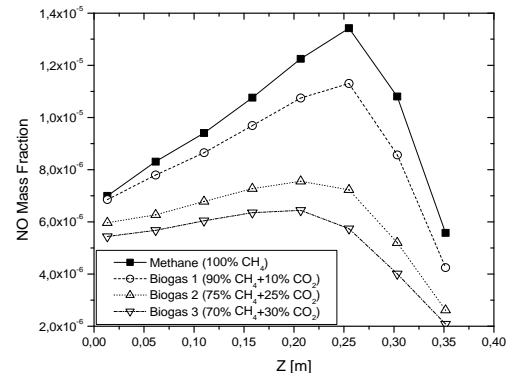
Fig. 7. Distribution of NO mass fraction.

An analysis of CO_2 distribution in the combustion chamber in the axis the combustor was carried for methane pure and mixture of methane and CO_2 (Fig. 8). The proper selection of a swirler is required to reduce the emission which can be concluded from the emission of NO and CO_2. The air at the secondary inlet is introduced to reduce the NO emission and also to mitigate CO_2 emission from natural gas.
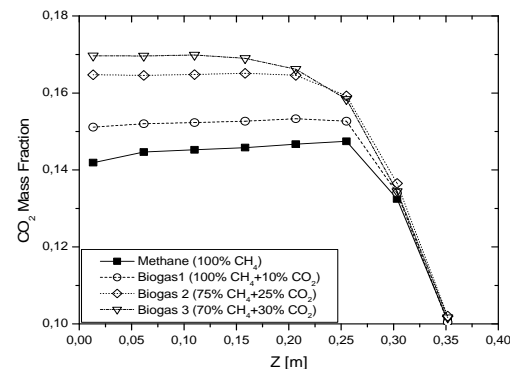
Fig. 8. Distribution of CO_2 mass fraction.

3.5 Analysis of Temperature Contours

Contours of the temperature in midaxil vertical plan have been plotted in Fig. 9. However, due to the dilution of burned mixture gas with the air, the gas mixture temperature is lower in primary zone. It can be seen from Fig. 10, the high temperature zone becomes bigger as the % CO_2 increases. It is because more fuel is burned in the combustor under the high % CO_2. Adding about 10% of CO_2 to methane lowers the adiabatic temperature of combustion by about 20K, and increasing the ratio of CO_2 to 40% by about 45K. Increasing the amount of carbon dioxide in the fuel leads to

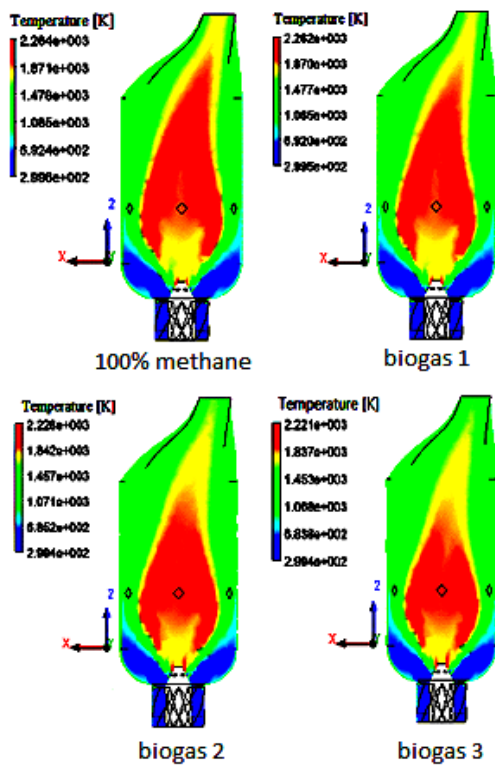lowering of the maximum combustion temperature.

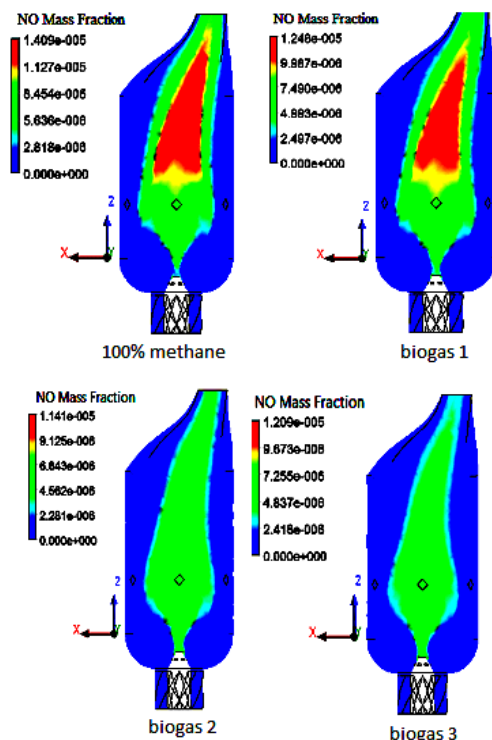Fig. 9. Temperature distribution in center plan.

Fig. 10. NO Mass fraction distribution.

3.6 Analysis of NO Contours

Contours of the NO mass fractions in mid-axial vertical plan have been plotted in Fig. 10. Profiles distribution of nitric oxide, they are formed in the combustion chamber in the case of the analyzed fuels. NO concentrations, however, are highest in the slow-moving, reverse-flowing fluid near the combustor centerline. The fluid here has had sufficient time to allow N_2 to react with O_2 and form NO. Pollution emission level from a combustor depends upon the interaction between the physical and chemical process and is strongly temperature dependent.

In thermal model, temperature controlled oxidation of N_2 leads to formation of NO whose emission level changes with axial distance. As temperature increases in the axial direction, oxidation of N_2 increases leading to increase in NO. Fig. 11 presents a set of measurements of toxic compounds or mixtures of natural gas (100% CH_4) and biogas 1, 2 and 3 burnt in strong swirl flows. The values measured for NO, CO and CO_2 correspond to those taken 30 mm from the rectangular shape outlet of the combustor which shows that the whole of NO emissions is produced no higher than the flame height indicated and that in the flame not burning of nitric oxides takes place.
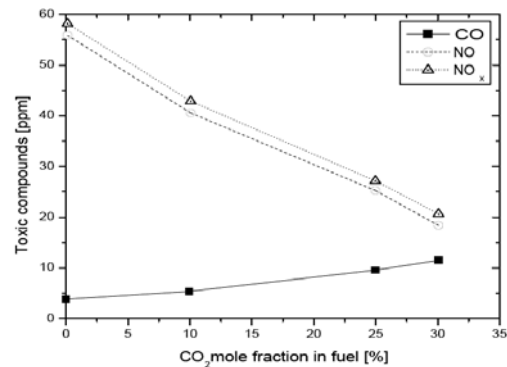

Fig. 11. Emission of NO, NO_x and CO taken 30 mm from the rectangular shape outlet of the combustor.

4. CONCLUSION

A turbulent swirling flow in a can-type gas turbine combustor model is modeled, applying, three-dimensional turbulence modeling procedures such as RANS-RSM. Quite satisfactory results have been obtained by the RANS-RSM approach for the gas turbine combustor can-type model. The analyses were carried out for diffusion chamber, using natural gas (100% CH_4) and biogas as fuels. Through the numerical simulations it was possible to notice that:

- CO_2 addition significantly improves flame stability and allows stable burner operation at the lean fuel/air ratios needed for reduced NO_x emissions, up to 30% CO_2 addition for NO_x reduction to the 33% competitive with current control technologies when both NO_x emissions and the cost of CO_2 removal are considered.

- The change in the fuel from natural gas to biogas changes the aerodynamic and thermal behavior significantly due to the variation of the

fuel mass flow, which is higher for the biogas, given that it has a lower heating value that the natural gas and different chemical composition as well

- The results of the investigation clearly demonstrate that it is possible to use such fuels in combustion systems with swirl burners.

REFERENCES

Ansys Fluent 14.0, Theory guid. http://www.ansys.com

Barnes, F. J., J. H. Bromly, T. J. Edwards and R. Madngezewsky (1988). NOₓ Emissions from Radiant Gas Burners. *Journal of the Institute of Energy. 155, 184-188.*

Baulch, D. L., D. D. Drysdall, D. G. Horne and A. C. Lloyd (1973). Evaluated Kinetic Data for High Temperature Reactions. 1, 2, 3. Butterworth.

Eldrainy, Y. A., J. Jeffrie and M. Jaafar (2008). Prediction of the flow inside a Micro Gas Turbine Combustor. *Journal of Mechanical* 25, 50-63.

Eymard, R., T. Gallouet and R. Herbin (2000). The Finite Volume Methode. *Handbook of Numerical Analysis 7, 713-1020.*

Fenimore, C. P. (1971). Formation of Nitric Oxide in Premixed Hydrocarbon Flames. In 13th Symp.(Int'l.) on Combustion. The Combustion Institute.

Franz, D. (2008*). An Introduction to the Theory of Fluid Flows*. Fluid Mechanics, Springer.

Fureby, C., F. F. G. L. Grinstein and E. J. Gutmark (2007). An experimental and computational study of a multi-swirl gas turbine combustor. *Proceedings of the Combustion Institute 31, 3107–3114.*

Ghenai, C. (2010). Combustion of Syngas Fuel in Gas Turbine Can Combustor. *Advances in Mechanical Engineering* 1, 1-13.

Gibson, M. M. and B. E. Launder (1978). Ground Effects on Pressure Fluctuations in the Atmospheric Boundary Layer. *J. Fluid Mech. 86, 491–511.*

Gohlke, O., T. Weber, P. Seguin and Y. Laborel (2010). A new process for NOx reduction in combustion systems for the generation of energy from waste. *Waste Management 30, 1348-1354.*

Launder, B. E. (1989). Second-Moment Closure: Present. and Future. Inter. J. Heat Fluid Flow 10(4), 282-300.

Launder, B. E., G. J. Reece and W. Rodi (1975). Progress in the Development of a Reynolds-Stress Turbulence Closure. *J. Fluid Mech. 68(3), 537–566.*

Lysenko D. A. and A. A. Solomatnikov (2003).

Numerical modeling of turbulent heat exchange in the combustion chambers of gas-turbine plants with the use of the Fluent package. *Journal of Engineering Physics and Thermophysics 76(4).*

Lysenko D. A. and A. A. Solomatnikov (2006). Numerical analysis of aerodynamics and hydraulic loss in the GTE′-150 combustion chamber of gas-turbine power plant with the use of the Fluent suite. *Journal of Engineering Physics and Thermophysics 79(4).*

Magnussen, B. F. (2005). The eddy dissipation concept a bridge between science and technology. *In ECCOMAS Thematic Conference on Computational Combustion*, Lisbon (Portugal).

Marzougui, H., F. Radhia, Z. Jihene and T. Lili (2015). Second Order Model for Strongly Sheared Compressible Turbulence. *Journal of Applied Fluid Mechanics 8(1), 113-121.*

Palash, S. M., M. A. kalam, H. H. Masjuki, I. M. Rizwanul Fattah and M. Mofijur (2013). Impact of biodiesel Combustion on NOx emissions and their reduction approaches. *J. Renewable and Sustainably Energy reviews 23, 473-490.*

Palm, R., S. Grundmanna, M. Weismüllera, S. Šarića, S. Jakirlić and C. Tropeaa (2006). Experimental characterization and modeling of inflow conditions for a gas turbine swirl combustor. *International Journal of Heat and Fluid Flow 27, 924-936.*

Patankar, S. V. (1983). *Numerical Heat Transfer and Fluid Flow*. McGraw-Hill, New York, USA.

Pathan, H., K. Partel and V. Tadvi (2012). Numerical Investigation of the Combustion of Methane-air Mixture in Gas Turbine can-type combustion chamber. *International Journal of Scientific and Engineering Research* 3(10), 1-7.

Rossignoli, P. (2010). High dust selective catalytic NOx reduction at WTE plants in Brescia. *In: 2nd International Conference on Biomass and Waste Combustion, Oslo.*

Sarkar S., C. G. Speziale and T. B. Gatski (1991). Modeling the Pressure-Strain Correlation of Turbulence. *Journal of fluid Mechanics 227, 245-272.*

Sarkar, S. (1995). The stabilizing effect of compressibility in turbulent shear flow . *Journal of fluid Mechanics 282, 163.*

Soete, G. G. D. (1974). Overall Reaction Rates of NO and N₂ Formation from Fuel Nitrogen. *Proceedings of the Combustion Institute 15, 1093–1102.*

Westbrook, C. and F. Dryer (1984). Chemical Kinetic Modeling of Hydrocarbon Combustion. *Progress in Energy and Combustion Science 10, 1-57.*

Westenberg, A. A. (1971). Comb. Sci. Tech. 4, 59.

White, M., S. Goff, S. Deduck and O. Gohlke (2009). New process for achieving very low NOx. *In: Proceedings of NAWTEC17-2372, 18-20 May, Chantilly, Virginia, USA.*

Widenhorn, A., B. Noll and M. Aigner (2009). Numerical characterization of the reacting flow in a swirled gas turbine model Combustor. *high performance computing in science and Engineering 8(5), 365-380.*

Widenhorn, A., B. Noll and M. Aigner (2010). Numerical characterization of a gas turbine model combustor *high performance computing in science and engineering 9(4), 179-195.*

Zeldovich, J. (1946). The oxidation of nitrogen in combustion explosions. *Acta Physico-chim. U.R.S.S. 21, 577-628.*